Time-Reversal-Even Nonlinear Current Induced Spin Polarization

Cong Xiao,[1,2,*,†] Weikang Wu,[3,*] Hui Wang,[4,*] Yue-Xin Huang,[4,*] Xiaolong Feng,[4] Huiying Liu,[5,4,‡]
Guang-Yu Guo,[6,7,§] Qian Niu,[8] and Shengyuan A. Yang[4]

[1]*Department of Physics, The University of Hong Kong, Hong Kong, People's Republic of China*
[2]*HKU-UCAS Joint Institute of Theoretical and Computational Physics at Hong Kong, Hong Kong, China*
[3]*Key Laboratory for Liquid-Solid Structural Evolution and Processing of Materials, Ministry of Education, Shandong University,
Jinan 250061, People's Republic of China*
[4]*Research Laboratory for Quantum Materials, Singapore University of Technology and Design, Singapore 487372, Singapore*
[5]*School of Physics, Beihang University, Beijing 100191, China*
[6]*Department of Physics, National Taiwan University, Taipei 10617, Taiwan, Republic of China*
[7]*Physics Division, National Center for Theoretical Sciences, Taipei 10617, Taiwan, Republic of China*
[8]*School of Physics, University of Science and Technology of China, Hefei, Anhui 230026, People's Republic of China*

We propose a time-reversal-even spin generation in second order of electric fields, which dominates the current induced spin polarization in a wide class of centrosymmetric nonmagnetic materials, and leads to a novel nonlinear spin-orbit torque in magnets. We reveal a quantum origin of this effect from the momentum space dipole of the anomalous spin polarizability. First-principles calculations predict sizable spin generations in several nonmagnetic hcp metals, in monolayer $TiTe_2$, and in ferromagnetic monolayer $MnSe_2$, which can be detected in experiment. Our work opens up the broad vista of nonlinear spintronics in both nonmagnetic and magnetic systems.

Nonlinear responses of solids are attracting great interest in recent research [1,2]. They dominate in crystals where the linear response is symmetry forbidden, probe novel band geometric quantities, and offer new tools to characterize and control material properties. For example, recent studies on various nonlinear anomalous Hall effects have connected them to intriguing geometric quantities such as Berry curvature dipole [3–5] and Berry connection polarizability [6–8], and revealed their utility to extract Néel vector [9–11] and to detect nontrivial band topologies [12,13].

In the field of spintronics, current induced spin polarization (CISP) is the central effect that enables electric control of spin degree of freedom [14,15]. In this context, one usually distinguishes contributions according to their parities under time reversal ($\mathcal{T}$), i.e., under the reversal of all magnetic moments in the system [15–17] (see Fig. 1). Clearly, the $\mathcal{T}$-odd part is present only in magnets, whereas the $\mathcal{T}$-even CISP exists in both magnetic and nonmagnetic systems [18–21]. It was shown that they give rise to two basic types of spin-orbit torques, allowing electrical manipulation of magnetic order parameters [15–17,22–31]. Previous studies focused on the linear CISP, which is limited to systems with inversion symmetry ($\mathcal{P}$) breaking. This left out the large family of $\mathcal{P}$ symmetric materials, in which the leading CISP is necessarily of nonlinear character. Recently, the $\mathcal{T}$-odd second-order nonlinear CISP was proposed in Ref. [32]. However, the corresponding $\mathcal{T}$-even part has not been investigated yet. As mentioned,

the $\mathcal{T}$-even nonlinear CISP occurs in even wider range of material systems, including also the nonmagnetic materials, many of which are technologically important (such as the elemental metals).

In this work, we study a special type of such a $\mathcal{T}$-even nonlinear CISP. It has a quantum origin arising from the *anomalous spin*, which is spotlighted here as a basic property of spin-orbit-coupled electrons under an electric field and can be expressed in terms of an intrinsic band geometric quantity which is called the anomalous spin polarizability (ASP). We show that the $\mathcal{T}$-even nonlinear spin response is determined by the momentum space dipole of ASP over the occupied states. We clarify the symmetry character of this effect and find that in several magnetic
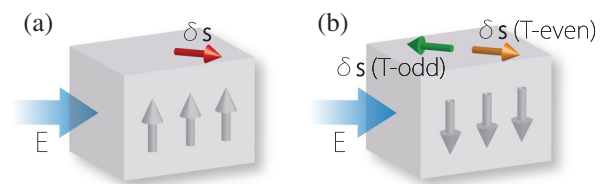

FIG. 1. Schematic figure showing the difference between $\mathcal{T}$-even and $\mathcal{T}$-odd CISPs. (a) Applied E field generates spin polarization δs. Gray arrows denote the (background) local magnetic moments in the material. (b) Under the reversal of local moments, the $\mathcal{T}$-even CISP is unchanged, whereas the $\mathcal{T}$-odd CISP flips sign. In nonmagnetic systems, only $\mathcal{T}$-even CISP exists.

crystal classes, the $\mathcal{T}$-even and $\mathcal{T}$-odd contributions give orthogonal spin polarizations, hence their effects can be readily separated in experiment. Combining our theory with first-principles calculations, we report sizable nonlinear spin generations in a number of nonmagnetic elemental metals, in monolayer TiTe$_2$, and in ferromagnetic monolayer MnSe$_2$. Our finding establishes the $\mathcal{T}$-even nonlinear CISP as a fundamental spintronic effect, which renders a new nonlinear spin-orbit torque in centrosymmetric magnets.

Symmetry characters.—Let us first understand the emergence of $\mathcal{T}$-even nonlinear CISP from the symmetry perspective. The quadratic spin polarization response δs to an applied electric field can be expressed as

$$\delta s_a = \alpha_{abc} E_b E_c, \tag{1}$$

where α is the nonlinear response tensor, the roman indices label the Cartesian components, and the Einstein summation convention is adopted. Obviously, in a $\mathcal{P}$-symmetric system, the linear response $\delta s \propto E$ is forbidden, and (1) becomes the leading effect.

α_{abc} can always be separated into a $\mathcal{T}$-even part and a $\mathcal{T}$-odd part: $\alpha = \alpha^{\text{even}} + \alpha^{\text{odd}}$. Note that in nonmagnetic materials, only α^{even} exists. The two parts have different symmetry properties. Here, we focus on α^{even}, which obeys the following symmetry transformation rule:

$$\alpha_{a'b'c'}^{\text{even}} = \det(\mathcal{R})\mathcal{R}_{a'a}\mathcal{R}_{b'b}\mathcal{R}_{c'c}\alpha_{abc}^{\text{even}}, \tag{2}$$

with $\mathcal{R}$ being a point group operation [33]. The obtained constraints are summarized in Table I.

From the analysis, we find that the $\mathcal{T}$-even nonlinear CISP is supported by 10 of the 11 centrosymmetric point groups, implying broad material platforms in which the effect could be dominating. The detailed forms of $\alpha_{abc}^{\text{even}}$ tensor constrained by symmetry are presented in the

TABLE I. Constraints on $\alpha_{a(bc)}^{\text{even}} = (\alpha_{abc}^{\text{even}} + \alpha_{acb}^{\text{even}})/2$ from magnetic point group symmetries. "✓" ("✗") means that the element is symmetry allowed (forbidden). Symmetry operations $\mathcal{RT}$ and $\mathcal{R}$ impose the same constraints. For simplicity, we assume the E field is applied within the xy plane.

	$\mathcal{P}$	C_2^z	C_3^z, S_6^z	$C_{4,6}^z$, S_4^z	$C_{2,4,6}^x$, S_4^x	C_3^x, S_6^x	σ_z	σ_x
$\alpha_{xxx}^{\text{even}}$	✓	✗	$-\alpha_{xyy}^{\text{even}}$	✗	✓	✓	✗	✓
$\alpha_{x(xy)}^{\text{even}}$	✓	✗	$\alpha_{yxx}^{\text{even}}$	✗	✗	✗	✗	✗
$\alpha_{xyy}^{\text{even}}$	✓	✗	✓	✗	✓	✓	✗	✓
$\alpha_{yxx}^{\text{even}}$	✓	✗	✓	✗	✗	✗	✗	✗
$\alpha_{y(xy)}^{\text{even}}$	✓	✗	$\alpha_{xyy}^{\text{even}}$	✗	✓	✓	✗	✓
$\alpha_{yyy}^{\text{even}}$	✓	✗	$-\alpha_{yxx}^{\text{even}}$	✗	✗	✓	✗	✗
$\alpha_{zxx}^{\text{even}}$	✓	✓	✓	✓	✗	✗	✓	✗
$\alpha_{z(xy)}^{\text{even}}$	✓	✓	✗	✗	✓	✓	✓	✓
$\alpha_{zyy}^{\text{even}}$	✓	✓	$\alpha_{zxx}^{\text{even}}$	$\alpha_{zxx}^{\text{even}}$	✗	✓	✓	✗

Supplemental Material [34]. Importantly, we find that in $\bar{6}m'2'$, $4/mm'm'$, $6/mm'm'$, and $\bar{3}m'$ magnetic groups, which do not support the linear CISP, the nonlinear CISPs due to $\mathcal{T}$-even and $\mathcal{T}$-odd parts must be along orthogonal directions for any direction of the driving electric field [34], thus allowing an easy separation of the two parts.

ASP dipole mechanism.—The spin density is given by the integral of the spin polarization $s^n(\boldsymbol{k})$ carried by each electron wave packet weighted by the distribution function $f_n(\boldsymbol{k})$ (we set $e = \hbar = 1$):

$$\boldsymbol{s} = \int [d\boldsymbol{k}] f_n(\boldsymbol{k}) \boldsymbol{s}^n(\boldsymbol{k}), \tag{3}$$

where n and $\boldsymbol{k}$ are the band index and the wave vector, respectively, and $[d\boldsymbol{k}]$ is shorthand for $\sum_n d\boldsymbol{k}/(2\pi)^d$ with d being the dimension of the system. The $\mathcal{T}$-even response requires a distribution function that breaks the occupation symmetry at $\boldsymbol{k}$ and $-\boldsymbol{k}$, otherwise it would vanish in nonmagnetic systems due to the Kramers degeneracy. This is provided by the nonequilibrium distribution computed to the first order of the driving E field. Using the Boltzmann equation with the constant relaxation time approximation, we have $f_n = f_0 - \tau E_c \partial_c f_0$, where f_0 is the equilibrium Fermi distribution, τ is the relaxation time, and $\partial_c \equiv \partial_{k_c}$. Meanwhile, with spin-orbit coupling, $\boldsymbol{s}^n(\boldsymbol{k})$ of a wave packet also acquires a correction by the E field [47]:

$$s_a^n(\boldsymbol{k}) = \langle u_n(\boldsymbol{k})|\hat{s}_a|u_n(\boldsymbol{k})\rangle + \Upsilon_{ab}^n(\boldsymbol{k})E_b, \tag{4}$$

where the first term is the expectation value of the spin operator for the eigenstate $|u_n(\boldsymbol{k})\rangle$, and the second term is the *anomalous spin* correction linear in the electric field. The coefficient of the correction,

$$\Upsilon_{ab}^n(\boldsymbol{k}) = 2\text{Im} \sum_{n' \neq n} \frac{s_a^{nn'}(\boldsymbol{k}) v_b^{n'n}(\boldsymbol{k})}{[\varepsilon_n(\boldsymbol{k}) - \varepsilon_{n'}(\boldsymbol{k})]^2}, \tag{5}$$

is the ASP, an intrinsic band geometric quantity representing the polarizability of anomalous spin to the applied E field. In (5), $\varepsilon_n(\boldsymbol{k})$ is the band energy, and the numerator involves the interband matrix elements of spin and velocity operators.

Substituting the expressions of f_n and (4) into (3) and collecting the $\mathcal{T}$-even terms of E^2 order, we obtain the nonlinear CISP response tensor

$$\alpha_{abc}^{\text{even}} = \tau \mathcal{D}_{abc}, \tag{6}$$

with

$$\mathcal{D}_{abc} = \int [d\boldsymbol{k}] f_0 \partial_c \Upsilon_{ab}^n \tag{7}$$

being the momentum space dipole moment of ASP over all occupied states in equilibrium. One checks that this is indeed a $\mathcal{T}$-even pseudotensor complying with the

symmetry analysis. It is a Fermi surface property as can be seen via an integration by parts in (7).

Our result shows that the $\mathcal{T}$-even nonlinear CISP is proportional to the ASP dipole. This is analogous to the $\mathcal{T}$-even nonlinear anomalous Hall effect in Ref. [3], which is proportional to the Berry curvature dipole. In fact, the expression of ASP [Eq. (5)] is also similar to the Berry curvature tensor Ω_{ab} [48], with one of the velocity matrix element replaced by the spin matrix element. The analogy can be further exemplified by comparing Eq. (4) with the well-known semiclassical equation of motion: $\dot{r}_a^n = v_a^{nn} + \Omega_{ab} E_b$ [48–50]. One directly observes that the anomalous spin parallels the anomalous velocity $\Omega_{ab} E_b$. Moreover, while integrating the anomalous velocity over occupied states gives the intrinsic linear anomalous Hall effect, the integration of anomalous spin also produces the intrinsic linear CISP [23,24,30]. This highlights the significance of anomalous spin (and ASP) as an essential ingredient in the description of spin-orbit-coupled Bloch electrons.

A model study.—To illustrate the features of ASP dipole and the resulting CISP, we first apply our theory to a modified Kane-Mele model defined on a buckled two-dimensional (2D) honeycomb lattice [Fig. 2(a)] [51–53], which reads

$$H = -t\sum_{\langle ij \rangle \sigma} c_{i\sigma}^\dagger c_{j\sigma} + it_{so}\sum_{\langle\langle ij \rangle\rangle \sigma\sigma'} \nu_{ij} c_{i\sigma}^\dagger s_{\sigma\sigma'}^z c_{j\sigma'}$$
$$- it_R \sum_{\langle\langle ij \rangle\rangle \sigma\sigma'} \mu_{ij} c_{i\sigma}^\dagger (s \times d_{ij})_{\sigma\sigma'}^z c_{j\sigma'}. \qquad (8)$$

Here $c_{i\sigma}$ ($c_{i\sigma}^\dagger$) is the annihilation (creation) operator for an electron with spin σ at site i. The first term is the nearest neighbor hopping. The second term is the intrinsic spin-orbit coupling in second neighbor hopping, where $\nu_{ij} = +(-)$ if the electron makes a left (right) turn during hopping from j to i. The third term is the intrinsic Rashba spin-orbit coupling due to lattice buckling, where d_{ij} is the unit vector pointing from site j to i. This term is needed to lower the symmetry from D_{6h} to D_{3d}, such that a nonlinear spin polarization can be induced by an *in-plane E* field.

According to Table I, the symmetries C_3^z, C_2^x, and σ_x of D_{3d} group enforce the following relations on α^{even}: $\alpha_{xyy}^{\mathrm{even}} = \alpha_{y(xy)}^{\mathrm{even}} = -\alpha_{xxx}^{\mathrm{even}}$. It follows that the system only allows an in-plane spin polarization in the form of

$$(\delta s_x, \delta s_y) = \alpha_{xxx}^{\mathrm{even}}(\cos 2\phi, -\sin 2\phi)E^2. \qquad (9)$$

Interestingly, the result is determined by a single independent element $\alpha_{xxx}^{\mathrm{even}}$, and exhibits an angular dependence with π periodicity. Here, ϕ is the polar angle of the in-plane E field measured from the C_2^x axis.

In Figs. 2(c)–2(f), we plot in the Brillouin zone the distribution of ASP as well as the k-resolved ASP dipole,
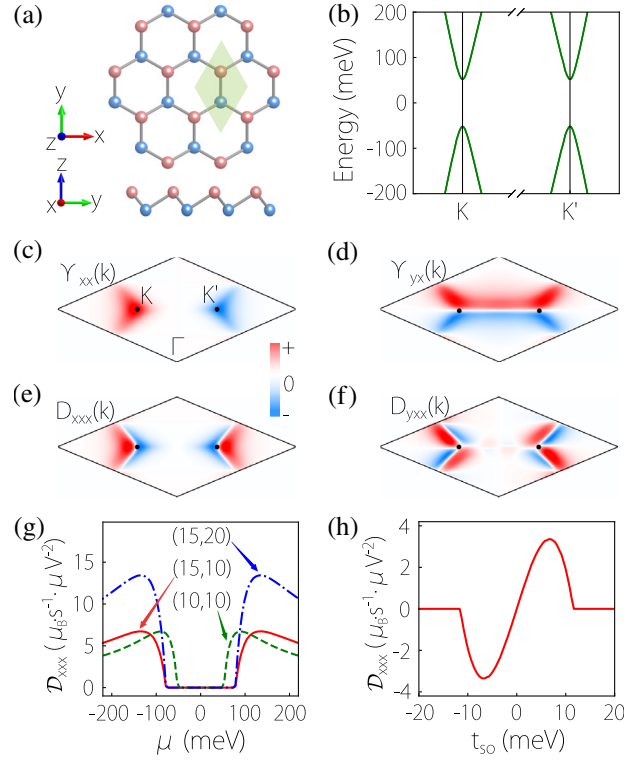

FIG. 2. (a) Top and side views of the buckled honeycomb lattice for the modified Kane-Mele model. (b) Low-energy bands for this model, with two valleys at K and K'. Here, we take $t = 0.85$ eV, $t_{so} = 10$ meV, and $t_R = 10$ meV. (c)–(f) show the k-space distribution of the ASP (c) Υ_{xx}, (d) Υ_{yx} and the k-resolved ASP dipole (e) $D_{xxx}(k)$ and (f) $D_{yxx}(k)$ for the valence band. (g) Calculated ASP dipole $\mathcal{D}_{xxx}$ versus the chemical potential μ. The legends denote (t_{so}, t_R) in units of meV. (h) $\mathcal{D}_{xxx}$ versus t_{so}, for $\mu = -60$ meV and $t_R = 10$ meV.

i.e., $D_{abc}(k) = \sum_n f_0 \partial_c \Upsilon_{ab}^n$, the integrand of (7). One observes that these quantities are concentrated around the small-gap region in the band structure, reflecting the interband coherence nature of band geometric quantities. Here, $D_{yxx}(k)$ is odd in k_y, whereas $D_{xxx}(k)$ is even, resulting in a nonvanishing ASP dipole $\mathcal{D}_{xxx}$. In Fig. 2(g), we plot $\mathcal{D}_{xxx}$ versus the chemical potential μ, which shows that the ASP dipole is enhanced around the band edges. In Fig. 2(h), we further see that $\mathcal{D}_{xxx}$ flips its sign with the spin-orbit coupling t_{so}.

Application to nonmagnetic metals.—Next, we ask if the $\mathcal{T}$-even nonlinear CISP is appreciable in real materials. Combining our theory with first-principles calculations, we first evaluate the effect in several hcp nonmagnetic transition metals, as listed in Table II, which have served as a main platform for studying the spin Hall effect [54]. These materials forbid the linear CISP because of their inversion symmetry.

Take the x/z to be along the crystal a/c axis, the D_{6h} point group dictates only one nonzero independent element

TABLE II. Calculated ASP dipole and CISP of some hcp transition metals at room temperature (RT). The RT transport relaxation time τ is obtained by using experimental resistivity data [55] and calculated Drude weight. The driving electric field is taken as $E = 10^5$ V/m [22,56,57].

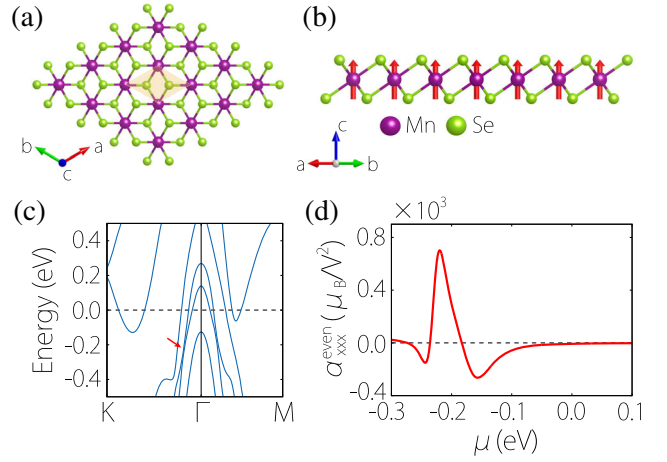| System	$\mathcal{D}_{y(zx)}$ 10^{18} $(\mu_B/\text{cm}^3)[\text{s(V/m)}^2]^{-1}$	δs_y 10^{-7} (μ_B/nm^3)	τ (10 fs)
Ti	-0.50	-0.43	0.85
Zr	1.69	1.34	0.79
Hf	-0.73	-0.80	1.10
Re	-0.93	-0.60	0.64
Ru	-1.18	-1.00	0.85

FIG. 3. (a) Top and (b) side views of the structure of monolayer $MnSe_2$. (c) Calculated band structure for monolayer $MnSe_2$ in the ferromagnetic phase. (d) Calculated $\alpha_{xxx}^{\text{even}}$ versus the chemical potential.

of ASP dipole $\mathcal{D}_{y(xz)}$, and the induced spin polarization must take the form of

$$\delta s = \alpha_{y(xz)}^{\text{even}} \sin 2\theta(-\sin\phi, \cos\phi, 0)E^2, \qquad (10)$$

lying in the xy plane, where θ and ϕ are spherical angles for the E field. Notably, δs is always normal to the field, and has a 2π periodicity in ϕ and a π periodicity in θ. For instance, if the E field is applied within the zx plane, the induced spin is along the y axis and reads $\delta s_y = \alpha_{y(xz)}^{\text{even}} \sin 2\theta E^2$, which reaches its maximum magnitude when $\theta = \pi/4$ and $3\pi/4$.

The results of $\mathcal{D}_{y(xz)}$ and δs_y from our first-principles calculations (calculation details in [34]) are shown in Table II. The induced spin density can reach 10^{-7} μ_B/nm^3 at $E = 10^5$ V/m, which is considerable compared to the linear CISP ($\sim 10^{-9}$ to 10^{-8} μ_B/nm^3) that has been measured in non-centrosymmetric nonmagnetic systems in previous experiments [58,59]. In the Supplemental Material [34], we also show the result for a 2D $\mathcal{P}$-symmetric nonmagnetic metal, the experimentally synthesized monolayer $TiTe_2$ [60], which shows nonlinear CISP of a similar magnitude.

Application to ferromagnetic 2D $MnSe_2$.—Our second example is the monolayer 1T-$MnSe_2$, which has been synthesized in recent experiment and demonstrated to be a room-temperature 2D ferromagnetic metal [61,62]. Its lattice structure is shown in Figs. 3(a) and 3(b), where each Mn atom is located at an inversion center, and the lattice point group is D_{3d}. Previous experiment [61] showed that the magnetization is out-of-plane (along z), so the magnetic point group is $\bar{3}m'$. Again, in this system, the linear CISP is forbidden by $\mathcal{P}$, thus the nonlinear effect dominates. The CISP constrained by symmetry takes the same form as Eq. (9). Thus, for an in-plane E field, the CISP is also in-plane and hence normal to the equilibrium magnetization.

The calculated band structure is plotted in Fig. 3(c). Figure 3(d) shows the variation of $\alpha_{xxx}^{\text{even}}$ with respect to the Fermi energy μ. As there has been no reported values for the relaxation time in monolayer $MnSe_2$, we take τ as 0.05 ps, a typical value for 2D metals at low temperatures [4]. Then, $\alpha_{xxx}^{\text{even}}$ is found to be ~ -7.1 μ_B/V^2 without doping, and is greatly enhanced upon hole doping, reaching $\sim 7 \times 10^2$ μ_B/V^2 at $\mu = -0.22$ eV as a result of the small local gap (about 15 meV), as marked by the red arrow in Fig. 3(c). In practice, such a doping level can be achieved in 2D materials by electric gating [4,63].

Under a moderate driving field of 10^5 V/m [22,56,57], the $\mathcal{T}$-even nonlinear CISP can reach $\sim 0.7 \times 10^{-5}$ μ_B/nm^2 (or 2.5×10^{-5} μ_B/nm^3 considering the monolayer thickness). Previous experiments showed that the linear CISP with much smaller magnitude, e.g., $\sim 10^{-9}$ to 10^{-6} μ_B/nm^3, can be measured in ferromagnets by magneto-optical or anisotropic magnetoresistance effects and can drive magnetization dynamics [22,26,30]. Thus, the predicted effect here is indeed significant. It should be readily detectable and can produce sizable spin-orbit torques.

In magnets, the $\mathcal{T}$-odd nonlinear CISP may also be present [32], which can be at the zeroth or the second order of τ. In experiment, such contributions can be distinguished from the $\mathcal{T}$-even effect here by their different τ scaling (e.g., by plotting against the longitudinal conductivity with varying temperature) [5,7]. Another way to separate them is to utilize their different symmetry properties. As mentioned, for the $\bar{3}m'$ group, to which the ferromagnetic 2D $MnSe_2$ belongs, the $\mathcal{T}$-even and $\mathcal{T}$-odd CISPs are always orthogonal (see the Supplemental Material [34]). For example, with E field along x, the $\mathcal{T}$-even CISP is along x, whereas the $\mathcal{T}$-odd CISP is in the yz plane. This permits an easy separation of the two effects [15].

Discussion.—We have proposed the $\mathcal{T}$-even nonlinear CISP effect and revealed its geometric origin in the ASP dipole. It offers a new mechanism for electric control of spin in $\mathcal{P}$-symmetric nonmagnetic materials and for driving

spin-orbit torques in ferromagnets. We demonstrate the first-principles evaluation of the effect for concrete non-magnetic and ferromagnetic materials, with sizable results well within the capacity of experiments. The study can be naturally extended to other materials. From our result, the effect should be favored in materials with band near degeneracies around Fermi level and with strong spin-orbit coupling for the low-energy states.

As mentioned, the ASP dipole mechanism for the nonlinear CISP parallels the Berry curvature dipole mechanism in the nonlinear anomalous Hall effect [3]. The relaxation time approximation is adopted here, so that the detailed disorder forms which are usually unknown do not pose a difficulty. Contributions beyond this approximation can be approached via semiclassical or quantum kinetic theories by assuming some specific form of disorder, in a way parallel to the study of the nonlinear Hall effect [64,65].

Besides CISP, there also exists current-induced orbital magnetization (OM). However, the theoretical description of OM is generally quite tricky [66–73]. Especially, how to formulate OM in nonequilibrium metallic states remains an open problem [72,73]. Some main difficulties of this problem are discussed in [34], and these are interesting topics to explore in future studies.

The spin polarization studied here is a spatially averaged quantity. In general, there can exist site-dependent spin [74] (and orbital [75]) polarization even in systems with preserved $\mathcal{P}$, as long as the site symmetry is low. Our theory can be extended to study such effects. This could be of particular interest for certain antiferromagnets [76], where the site-dependent CISP can induce a Néel torque to manipulate antiferromagnetism [15,17,77].

---

*These authors contributed equally to this work.
†congxiao@hku.hk
‡liuhuiying@pku.edu.cn
§gyguo@phys.ntu.edu.tw

[1] Q. Ma, A. G. Grushin, and K. S. Burch, Nat. Mater. **20**, 1601 (2021).

[2] Z. Z. Du, H.-Z. Lu, and X. Xie, Nat. Rev. Phys. **3**, 744 (2021).

[3] I. Sodemann and L. Fu, Phys. Rev. Lett. **115**, 216806 (2015).

[4] Q. Ma et al., Nature (London) **565**, 337 (2019).

[5] K. Kang, T. Li, E. Sohn, J. Shan, and K. F. Mak, Nat. Mater. **18**, 324 (2019).

[6] Y. Gao, S. A. Yang, and Q. Niu, Phys. Rev. Lett. **112**, 166601 (2014).

[7] S. Lai, H. Liu, Z. Zhang, J. Zhao, X. Feng, N. Wang, C. Tang, Y. Liu, K. S. Novoselov, S. A. Yang, and W.-b. Gao, Nat. Nanotechnol. **16**, 869 (2021).

[8] H. Liu, J. Zhao, Y.-X. Huang, X. Feng, C. Xiao, W. Wu, S. Lai, W.-b. Gao, and S. A. Yang, Phys. Rev. B **105**, 045118 (2022).

[9] D.-F. Shao, S.-H. Zhang, G. Gurung, W. Yang, and E. Y. Tsymbal, Phys. Rev. Lett. **124**, 067203 (2020).

[10] C. Wang, Y. Gao, and D. Xiao, Phys. Rev. Lett. **127**, 277201 (2021).

[11] H. Liu, J. Zhao, Y.-X. Huang, W. Wu, X.-L. Sheng, C. Xiao, and S. A. Yang, Phys. Rev. Lett. **127**, 277202 (2021).

[12] J. I. Facio, D. Efremov, K. Koepernik, J.-S. You, I. Sodemann, and J. van den Brink, Phys. Rev. Lett. **121**, 246403 (2018).

[13] S. Sinha, P. C. Adak, A. Chakraborty, K. Das, K. Debnath, L. D. V. Sangani, K. Watanabe, T. Taniguchi, U. V. Waghmare, A. Agarwal, and M. M. Deshmukh, Nat. Phys. **18**, 765 (2022).

[14] D. Awschalom, Physics **2**, 50 (2009).

[15] A. Manchon, J. Železný, I. M. Miron, T. Jungwirth, J. Sinova, A. Thiaville, K. Garello, and P. Gambardella, Rev. Mod. Phys. **91**, 035004 (2019).

[16] F. Freimuth, S. Blügel, and Y. Mokrousov, Phys. Rev. B **90**, 174423 (2014).

[17] J. Železný, H. Gao, A. Manchon, F. Freimuth, Y. Mokrousov, J. Zemen, J. Mašek, J. Sinova, and T. Jungwirth, Phys. Rev. B **95**, 014403 (2017).

[18] E. L. Ivchenko and G. E. Pikus, JETP Lett. **27**, 604 (1978).

[19] A. G. Aronov and Y. Lyanda-Geller, JETP Lett. **50**, 431 (1989).

[20] Y. M. Edelstein, Solid State Commun. **73**, 233 (1990).

[21] D. Culcer and R. Winkler, Phys. Rev. Lett. **99**, 226601 (2007).

[22] A. Chernyshov, M. Overby, X. Liu, J. K. Furdyna, Y. Lyanda-Geller, and L. P. Rokhinson, Nat. Phys. **5**, 656 (2009).

[23] I. Garate and A. H. MacDonald, Phys. Rev. B **80**, 134403 (2009).

[24] I. Garate and M. Franz, Phys. Rev. Lett. **104**, 146802 (2010).

[25] I. M. Miron, G. Gaudin, S. Auffret, B. Rodmacq, A. Schuhl, S. Pizzini, J. Vogel, and P. Gambardella, Nat. Mater. **9**, 230 (2010).

[26] D. Fang, H. Kurebayashi, J. Wunderlich, K. Výborný, L. P. Zârbo, R. P. Campion, A. Casiraghi, B. L. Gallagher, T. Jungwirth, and A. J. Ferguson, Nat. Nanotechnol. **6**, 413 (2011).

[27] I. M. Miron, K. Garello, G. Gaudin, P.-J. Zermatten, M. V. Costache, S. Auffret, S. Bandiera, B. Rodmacq, A. Schuhl, and P. Gambardella, Nature (London) **476**, 189 (2011).

[28] L. Liu, C.-F. Pai, Y. Li, H. W. Tseng, D. C. Ralph, and R. A. Buhrman, Science **336**, 555 (2012).

[29] K. Garello, I. M. Miron, C. O. Avci, F. Freimuth, Y. Mokrousov, S. Blügel, S. Auffret, O. Boulle, G. Gaudin, and P. Gambardella, Nat. Nanotechnol. **8**, 587 (2013).

[30] H. Kurebayashi, J. Sinova, D. Fang, A. Irvine, T. D. Skinner, J. Wunderlich, V. Novák, R. P. Campion, B. L. Gallagher, E. K. Vehstedt, L. P. Zârbo, K. Výborný, A. J. Ferguson, and T. Jungwirth, Nat. Nanotechnol. **9,** 211 (2014).

[31] C. Ciccarelli, L. Anderson, V. Tshitoyan, A. J. Ferguson, F. Gerhard, C. Gould, L. W. Molenkamp, J. Gayles, J. Železný, L. Šmejkal, Z. Yuan, J. Sinova, F. Freimuth, and T. Jungwirth, Nat. Phys. **12,** 855 (2016).

[32] C. Xiao, H. Liu, W. Wu, H. Wang, Q. Niu, and S. A. Yang, Phys. Rev. Lett. **129,** 086602 (2022).

[33] For α^{odd}, the right band side of (2) has an extra minus sign if $\mathcal{R}$ contains time reversal [32].

[34] See Supplemental Material at http://link.aps.org/supplemental/10.1103/PhysRevLett.130.166302 for the detailed matrix forms of $\alpha^{\text{even}}_{a(bc)}$ in all nonmagnetic and ferromagnetic point groups that forbid the linear CISP, the comparison of symmetry enforced forms of α^{even} and α^{odd} in such ferromagnetic point groups, the computational details in concrete materials, and brief discussions on existing theoretical difficulties about current-induced orbital magnetization, which includes Refs. [35–46].

[35] J. P. Perdew, K. Burke, and M. Ernzerhof, Phys. Rev. Lett. **77,** 3865 (1996).

[36] H. Ebert, Phys. Rev. B **38,** 9390 (1988).

[37] G. Y. Guo and H. Ebert, Phys. Rev. B **51,** 12633 (1995).

[38] O. K. Andersen, Phys. Rev. B **12,** 3060 (1975).

[39] W. Temmerman, P. Sterne, G. Guo, and Z. Szotek, Mol. Simul. **4,** 153 (1989).

[40] P. E. Blöchl, Phys. Rev. B **50,** 17953 (1994).

[41] G. Kresse and J. Hafner, Phys. Rev. B **49,** 14251 (1994).

[42] G. Kresse and J. Furthmüller, Phys. Rev. B **54,** 11169 (1996).

[43] S. L. Dudarev, G. A. Botton, S. Y. Savrasov, C. J. Humphreys, and A. P. Sutton, Phys. Rev. B **57,** 1505 (1998).

[44] N. Marzari and D. Vanderbilt, Phys. Rev. B **56,** 12847 (1997).

[45] I. Souza, N. Marzari, and D. Vanderbilt, Phys. Rev. B **65,** 035109 (2001).

[46] A. A. Mostofi, J. R. Yates, Y.-S. Lee, I. Souza, D. Vanderbilt, and N. Marzari, Comput. Phys. Commun. **178,** 685 (2008).

[47] L. Dong, C. Xiao, B. Xiong, and Q. Niu, Phys. Rev. Lett. **124,** 066601 (2020).

[48] D. Xiao, M.-C. Chang, and Q. Niu, Rev. Mod. Phys. **82,** 1959 (2010).

[49] M.-C. Chang and Q. Niu, Phys. Rev. Lett. **75,** 1348 (1995).

[50] G. Sundaram and Q. Niu, Phys. Rev. B **59,** 14915 (1999).

[51] C. L. Kane and E. J. Mele, Phys. Rev. Lett. **95,** 226801 (2005).

[52] C.-C. Liu, W. Feng, and Y. Yao, Phys. Rev. Lett. **107,** 076802 (2011).

[53] C.-C. Liu, H. Jiang, and Y. Yao, Phys. Rev. B **84,** 195430 (2011).

[54] F. Freimuth, S. Blügel, and Y. Mokrousov, Phys. Rev. Lett. **105,** 246602 (2010).

[55] C. Kittel, *Introduction to Solid State Physics*, 7th ed. (John Wiley and Sons, New York, 1996).

[56] K. Olejník, T. Seifert, Z. Kašpar, V. Novák, P. Wadley, R. P. Campion, M. Baumgartner, P. Gambardella, P. Němec, J. Wunderlich, J. Sinova, P. Kužel, M. Müller, T. Kampfrath, and T. Jungwirth, Sci. Adv. **4,** 3566 (2018).

[57] X. F. Zhou, X. Z. Chen, J. Zhang, F. Li, G. Y. Shi, Y. M. Sun, M. S. Saleem, Y. F. You, F. Pan, and C. Song, Phys. Rev. Appl. **11,** 054030 (2019).

[58] Y. K. Kato, R. C. Myers, A. C. Gossard, and D. D. Awschalom, Phys. Rev. Lett. **93,** 176601 (2004).

[59] N. P. Stern, S. Ghosh, G. Xiang, M. Zhu, N. Samarth, and D. D. Awschalom, Phys. Rev. Lett. **97,** 126603 (2006).

[60] P. Chen, W. W. Pai, Y.-H. Chan, A. Takayama, C.-Z. Xu, A. Karn, S. Hasegawa, M.-Y. Chou, S.-K. Mo, A.-V. Fedorov, and T.-C. Chiang, Nat. Commun. **8,** 1 (2017).

[61] D. J. O'Hara, T. Zhu, A. H. Trout, A. S. Ahmed, Y. K. Luo, C. H. Lee, M. R. Brenner, S. Rajan, J. A. Gupta, D. W. McComb, and R. K. Kawakami, Nano Lett. **18,** 3125 (2018).

[62] J. Vanherck, C. Bacaksiz, B. Sorée, M. V. Milošević, and W. Magnus, Appl. Phys. Lett. **117,** 052401 (2020).

[63] J. Chen, H. J. Qin, F. Yang, J. Liu, T. Guan, F. M. Qu, G. H. Zhang, J. R. Shi, X. C. Xie, C. L. Yang, K. H. Wu, Y. Q. Li, and L. Lu, Phys. Rev. Lett. **105,** 176602 (2010).

[64] Z. Z. Du, C. M. Wang, S. Li, H.-Z. Lu, and X. C. Xie, Nat. Commun. **10,** 3047 (2019).

[65] C. Xiao, Z. Z. Du, and Q. Niu, Phys. Rev. B **100,** 165422 (2019).

[66] T. Thonhauser, D. Ceresoli, D. Vanderbilt, and R. Resta, Phys. Rev. Lett. **95,** 137205 (2005).

[67] D. Xiao, J. Shi, and Q. Niu, Phys. Rev. Lett. **95,** 137204 (2005).

[68] J. Shi, G. Vignale, D. Xiao, and Q. Niu, Phys. Rev. Lett. **99,** 197202 (2007).

[69] A. Malashevich, I. Souza, S. Coh, and D. Vanderbilt, New J. Phys. **12,** 053032 (2010).

[70] K.-T. Chen and P. A. Lee, Phys. Rev. B **84,** 205137 (2011).

[71] T. Yoda, T. Yokoyama, and S. Murakami, Sci. Rep. **5,** 1 (2015).

[72] C. Xiao, H. Liu, J. Zhao, S. A. Yang, and Q. Niu, Phys. Rev. B **103,** 045401 (2021).

[73] C. Xiao, Y. Ren, and B. Xiong, Phys. Rev. B **103,** 115432 (2021).

[74] X. Zhang, Q. Liu, J.-W. Luo, A. J. Freeman, and A. Zunger, Nat. Phys. **10,** 387 (2014).

[75] J. H. Ryoo and C.-H. Park, NPG Asia Mater. **9,** e382 (2017).

[76] W. Chen, M. Gu, J. Li, P. Wang, and Q. Liu, Phys. Rev. Lett. **129,** 276601 (2022).

[77] J. Železný, H. Gao, K. Výborný, J. Zemen, J. Mašek, A. Manchon, J. Wunderlich, J. Sinova, and T. Jungwirth, Phys. Rev. Lett. **113,** 157201 (2014).